ELSEVIER

Materials Science and Engineering A349 (2003) 136–149

MATERIALS SCIENCE & ENGINEERING A

www.elsevier.com/locate/msea

Investigations on the fracture toughness of austempered ductile irons austenitized at different temperatures

P. Prasad Rao [a], Susil K. Putatunda [b,*]

[a] Department of Metallurgical and Materials Engineering, Karnatak Regional Engineering College, Surathkal, Karnataka State 574 157, India
[b] Department of Chemical Engineering and Materials Science, Wayne State University, 5050 Anthony Wayne Drive, Detroit, MI 48202, USA

Received 22 March 2002; received in revised form 6 September 2002

Abstract

Ductile cast iron was austenitized at four different temperatures and subsequently austempered at six different temperatures. Plane strain fracture toughness was evaluated under all the heat treatment conditions and correlated with the microstructural features such as the austenite content and the carbon content of the austenite. Fracture mechanism was studied by scanning electron microscopy. It was found that the optimum austempering temperature for maximum fracture toughness decreased with increasing austenitizing temperature. This could be interpreted in terms of the microstructural features. A study of the fracture mechanism revealed that good fracture toughness is unlikely to be obtained when austempering temperature is less than half of the austenitizing temperature on the absolute scale.

Keywords: Fracture toughness; Austempered ductile iron; Temperature

1. Introduction

Austempered ductile iron (ADI) has drawn considerable attention in the recent years because of its potential to replace heat-treated steels in many engineering applications [1–5]. It has many attractive properties such as an unusual combination of high strength and ductility, good wear resistance and high fatigue strength [6–11]. Its fracture toughness is comparable to those of quenched and tempered medium carbon and low alloy steels [12–17]. Besides, it has the advantage of lower material cost, lower production cost, lower density, better machinability, and higher damping capacity than the steels it is expected to replace. It is therefore not surprising that ADI has drawn so much attention in recent years.

The austempering heat treatment involves two steps. The sample is initially heated to a high temperature such that the matrix is fully austenitic (γ). It is then cooled rapidly to an intermediate temperature in the range of 250–450 °C and held at that temperature for the required length of time. Finally it is air cooled to room temperature. ADI has a unique microstructure consisting of ferrite (α) and high carbon austenite (γ_{HC}), rather than ferrite and iron carbide as in austempered steels. Because of this, the product of austempering reaction in ductile iron is called as 'ausferrite' rather than bainite as in steel. During the heat treatment cycle ADI undergoes a two-stage reaction process. In the first stage, the austenite decomposes into ferrite (α) and high carbon austenite (γ_{HC}):

$$\gamma_{HC} \rightarrow \alpha + \varepsilon \text{ (carbide)} \quad (1)$$

If the casting is held at the austempering temperature for too long, then a second reaction sets in, where the high carbon austenite further decomposes into ferrite and carbide:

$$\gamma \rightarrow \alpha + \gamma_{HC} \quad (2)$$

This second or stage II reaction is undesirabe because it embrittles the material and degrades the mechanical properties of ADI. The morphology of ferrite and austenite, their volume fractions, the carbon content of

* Corresponding author. Tel.: +1-313-577-3808; fax: +1-313-577-3810.
E-mail address: aa4597@wayne.edu (S.K. Putatunda).

0921-5093/02/$ - see front matter © 2002 Elsevier Science B.V. All rights reserved.
doi:10.1016/S0921-5093(02)00633-0

the austenite and their microstructural features depend on the heat treatment conditions. It is therefore very important to study the influence of the heat treatment parameters such as the austenitizing time and temperature and the austempering time and temperature on the evolution of the microstructure, and through that on the mechanical properties. Several investigators [18–21] have studied the correlation between the mechanical properties and the microstructure resulting from the changes in the austempering time and temperature. We now have a good understanding of this aspect. ADIs austempered at lower temperatures have high hardness, high strength and low ductility, while that austempered at higher temperatures exhibit lower hardness, lower strength and higher ductility. Thus it is found that strength decreases with increasing austempering temperature, while the ductility increases simultaneously. For a high tensile toughness, it is desirable to have an upper ausferritic microstructure [22] that consists of about 40 vol.% of austenite and broad blades of isolated ferrite.

The influence of the austenitizing temperature and time on the microstructure and mechanical properties have also been studied, but to a far lesser extent [20,22–24]. Increasing austenitizing temperature is known to increase the carbon content of the austenite, and thereby increase the volume fraction of austenite. Since most of the desirable properties of the ADI mentioned above are attributed to the presence of this high carbon stable austenite, it is desirable to maximize its amount in the microstructure. However, Rouns et al. [20] have shown that the driving force for the stage I process decreases with increasing austenitizing temperature. Due to this, at higher temperatures, there will be a considerable amount of martensite containing segregated regions at the prior austenite grain boundaries. Such a microstructure results in poor mechanical properties, and is not desired. Darwish et al. [23] have also reported similar results. Therefore, it is preferable to austenitize at a lower temperature. This will also give a refined microstructure. However, unduly decreasing the austenitizing temperature (T_γ) can result in lower strength because of an excessive reduction in the carbon content of the austenite.

Fracture toughness is an important parameter while designing structural components. It is important to understand the influence of the microstructure on the fracture toughness so that the heat treatment parameters can be optimized. It is known from previous investigations [18,19,24–28] that ADI with a lower ausferritic microstructure has generally better fracture toughness than that with an upper ausferritic microstructure. When the fracture toughness is plotted against the austempering temperature, it is found that the fracture toughness initially increases with increasing temperature, reaches a maximum at an intermediate temperature of around 300 °C and decreases with further increase in temperature. This is believed to be the result of interplay between the effects of ferrite grain size and the austenite volume fraction [27,28]. Ferrite has the maximum fracture toughness at the lowest austempering temperature, because it then has the finest grain size. On the other hand, the austenite content (X_γ) increases with austempering temperature. The contribution to fracture toughness from austenite, therefore, increases with increasing temperature. The actual toughness would be controlled by the weakest link, which is austenite at low temperatures, and ferrite at high temperatures. It has been shown [26,28] that the following relationship is valid in austempered ductile irons:

$$K_{IC}^2 = \sigma_y (X_\gamma C_\gamma)^{1/2} \quad (3)$$

where σ_y is the yield strength of ADI, X_γ is the volume fraction of austenite, and C_γ is the carbon content of the austenite. It is also known [29,30] that σ_y essentially depends on the width of the ferrite blade L, and varies as $L^{-1/2}$. While σ_y increases with decreasing austempering temperature, $X_\gamma C_\gamma$ increases with increasing austempering temperature. Therefore, a plot of K_{IC} against austempering temperature shows a maximum around 300 °C. The theoretical plot is shown to closely match with the experimental plot [28]. Therefore it can be concluded that the following microstructural features are necessary to obtain optimum fracture toughness in ADI:

a) lower ausferritic microstructure consisting of fine ferrite blades.
b) austenite content of around 25 vol.%.
c) a high carbon content of the austenite of more than 1.8 wt.%.

Besides the austempering temperature, an equally important parameter is the austenitizing temperature. However, there is rather very limited information available in literature on the influence of the austenitizing temperature on the fracture toughness of ADI. Klug et al. [31] studied the fracture toughness of samples austenitized at 1067, 982 and 897 °C, and subsequently austempered at 367 °C for 1 h. While the austenite content increased considerably with the increase in austenitizing temperature, tensile properties and fracture toughness were found to deteriorate. This was attributed to the embrittling effect of the austenite grain boundaries by the precipitation of phosphorus. Doong and Chen [32] investigated the fracture toughness of ADI after austenitizing at four different temperatures: 850, 900, 950 and 1000 °C. These were subsequently austempered for 4 h at 300 or 400 °C. When austempered at 300 °C, best fracture toughness as well as tensile properties were obtained in samples austenitized at 900 °C. All the samples showed uniformly low

Table 1
Chemical Composition of the iron (in wt.%)

C	3.54
Si	2.81
Mn	0.43
S	0.009
P	0.031
Mg	0.05
Cu	0.56
Ni	1.52
Mo	0.30
Cr	0.30

austenite content. When austempered at 400 °C the fracture toughness was still lower, and the austenite content was unusually low at less than 5 vol.%. It is likely that these samples were embrittled by carbide precipitation (second reaction in ADI) due to excessively long austempering periods.

Thus it can be seen that there is generally a lack of correlation between the microstructure and the fracture toughness of samples austenitized at different temperatures. Such a correlation is necessary in order to optimize the heat treatment parameters so that the fracture toughness can be maximized. Previous investigations [18,19,22,26–28] have clearly shown that the optimum microstructure for obtaining maximum tensile toughness and maximum fracture toughness are very different. While the former requires an upper ausferritic microstructure [26], the latter requires a lower ausferritic microstructure [22]. Therefore information on the influence of austenitizing temperature on tensile toughness cannot be extended to optimize the microstructure for maximizing the fracture toughness. It was therefore decided to take up a systematic investigation of the influence of austenitizing temperature on the microstructure, the tensile properties, and the fracture toughness of samples austempered at different temperatures.

2. Experimental procedure

The present investigation was carried out on a ductile iron of composition shown in Table 1. Round tensile samples and compact tension samples were machined from cast slabs as per ASTM standards E-8 [33] and E-399 [34]. These samples were austenitized for 2 h at 816, 871, 927 and 982 °C. These were subsequently austempered for 2 h at 260, 288, 302, 316, 357 and 385 °C. The morphology of the resulting microstructure was characterized by optical microscopy. The volume fraction of ferrite and austenite, as well as the carbon content of the austenite were estimated by X-ray diffraction technique using Rigaku rotating head diffractometer with crystal monochromated Cu K_α radiation. Tensile tests were carried out as per ASTM E-8 [33]

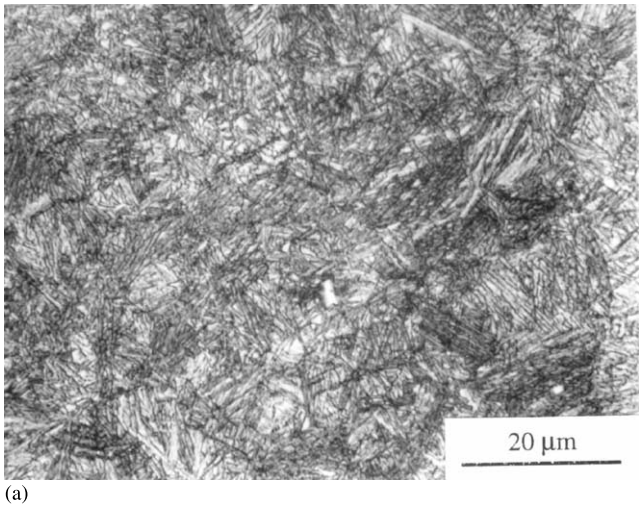

(a)

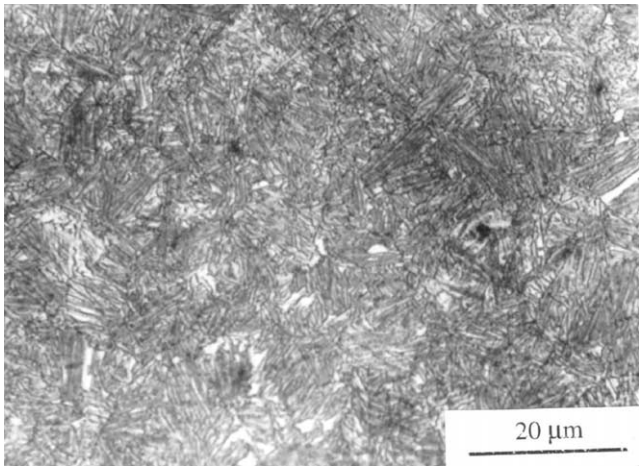

(b)

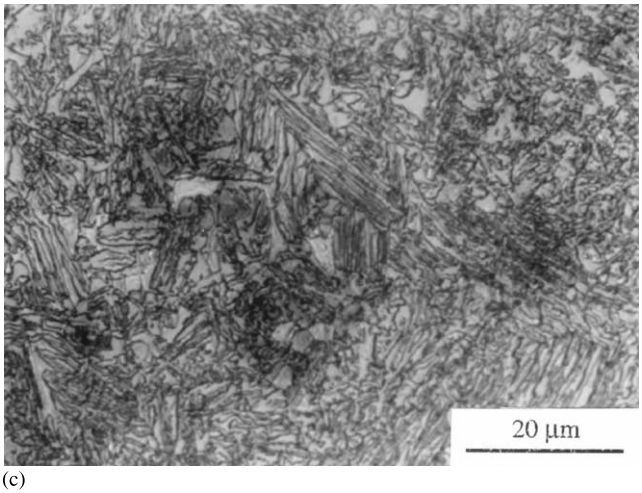

(c)

Fig. 1. (a) Microstructure of samples austenitized at 816 °C and austempered at 260 °C. (b) Microstructure of samples austenitized at 816 °C and austempered at 316 °C. (c) Microstructure of samples austenitized at 816 °C and austempered at 385 °C.

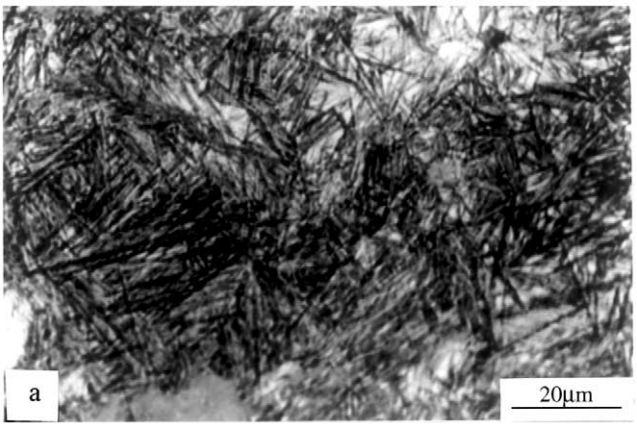

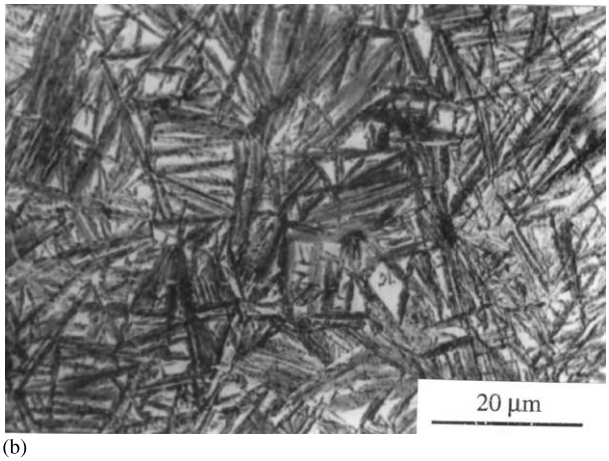

(b)

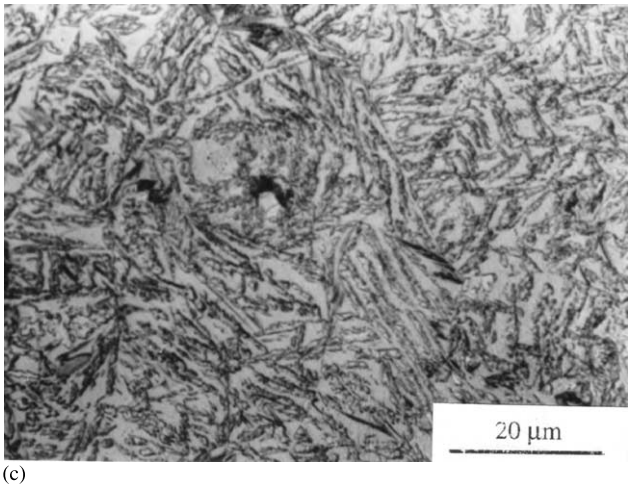

(c)

Fig. 2. (a) Microstructure of samples austenitized at 927 °C and austempered at 260 °C. (b) Microstructure of samples austenitized at 927 °C and austempered at 316 °C. (c) Microstructure of samples austenitized at 927 °C and austempered at 385 °C.

and the plain strain fracture toughness were determined as per ASTM standard E-399 [34] on an MTS 810 servohydraulic machine. The fracture surfaces of the fracture toughness samples were examined on a Hitachi S-2400 scanning electron microscope to elicit information on the fracture mechanism. The experimental details have been discussed in the earlier publications [22,26–28].

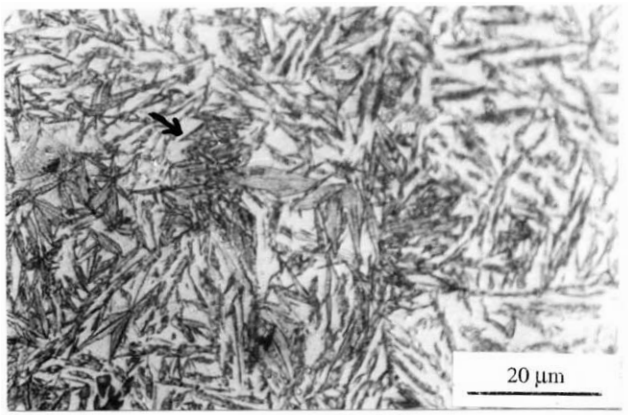

Fig. 3. Microstructure of samples austenitized at 982 °C and austempered at 385 °C. Arrow indicates strain induced martensite.

3. Results and discussion

3.1. Microstructure

Typical microstructures of the samples austenitized at 816 °C and then austempered at three different temperatures are shown in Fig. 1. When austempered at the lower temperatures of 260–316 °C, typically lower ausferritic microstructures were observed. These had very fine needles of ferrite with thin austenite regions present as slivers between them. Higher austempering temperatures resulted in typically upper ausferritic microstructures, which had broad ferrite needles. Broad blocky austenite regions generally separated these from each other. Similar microstructures were observed at higher austenitizing temperatures too. The length of the ferrite needles was generally found to increase with increasing austenitizing temperature. This can be noted by comparing the microstructures shown in Fig. 2, of the samples austenitized at 927 °C with those in Fig. 1. The increase in the length of the ferrite needles can be attributed to the greater coarsening of the austenite grains at the higher temperatures. The ferrite needles on nucleation grow till they encounter a barrier, which is the austenite grain boundary during early stages. The length of the largest ferrite needles can be assumed to represent the prior austenite grain size. This was found to increase with increasing austenitizing temperature.

It is known that ferrite nucleates at the graphite/austenite interface, and moves out towards the prior austenite grain boundary. Thus, in samples austenitized at higher temperatures, the growth occurs over longer distances. This, together with the fact that the carbon diffusion rates are lower because of the higher initial matrix carbon, results in considerable inhomogeneity,

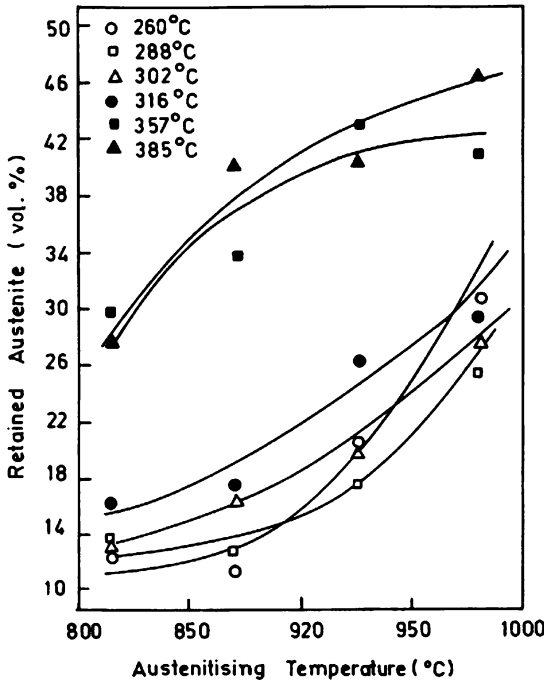

Fig. 4. Influence of the austenitizing temperature on the austenite content at different austempering temperatures.

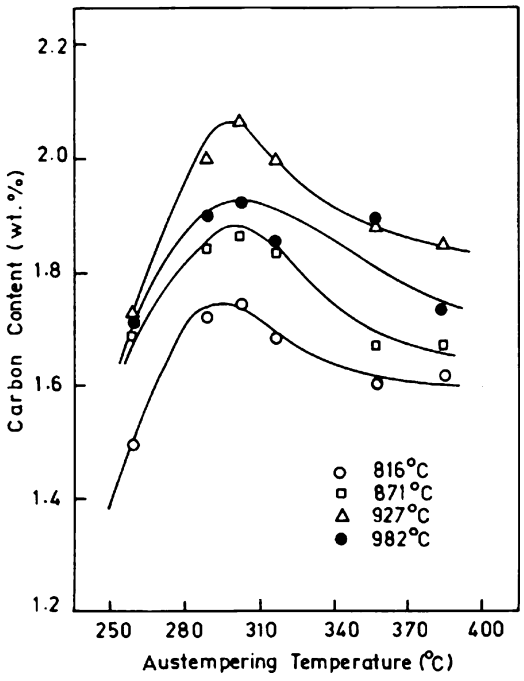

Fig. 5. Influence of the austempering temperature on the carbon content of the austenite at different austenitizing temperatures.

that manifests in the form of untransformed austenite at the prior austenite grain boundaries. This low carbon unstable austenite can transform to martensite on cooling from the austempering temperature. If not, it can transform to martensite on being subjected to a strain. This type of strain-induced transformation was observed in samples austenitized at the highest temperature of 982 °C. Fig. 3 shows clusters of martensite needles believed to have been formed from the unstable austenite during metallographic grinding operation. Besides the morphology, the other important microstructural features are the volume fractions of the ferrite and austenite, and the carbon content of the austenite. These were estimated by the X-ray diffraction technique.

The influence of the austenitizing temperature on the volume fraction of the austenite on austempering at different temperatures is shown in Fig. 4. It can be seen that at any austempering temperature, the austenite content increases with increasing austenitizing temperature. At the lower austempering temperatures (260–316 °C) the austenite content increases from an average of nearly 14 vol.% at 816 °C to a little over 28 vol.% at 982 °C. This signifies an increase of more than 100% on increasing the austenitizing temperature from 816 to 982 °C. Much of this increase occurs at the two higher austenitizing temperatures of 927 and 982 °C. The variation in the austenite content is rather marginal at the two lower austenitizing temperatures of 816 and 871 °C. The picture is quite different when one looks at the austempering temperatures of 357 and 385 °C. These had an average austenite content of 28 vol.% when austenitized at 816 °C, but an average of 44 vol.% when austenitized at 982 °C. This is an increase of only 50%, and much of this occurred at the lower austenitizing temperatures. Thus two distinct features are observed between the samples austempered at the lower temperatures and those at the higher temperatures. The

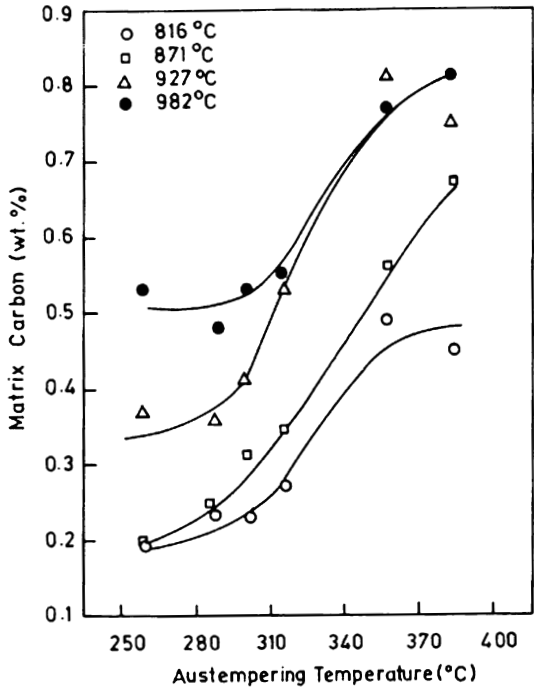

Fig. 6. Influence of the austempering temperature on the matrix carbon content of the austenite at different temperatures.

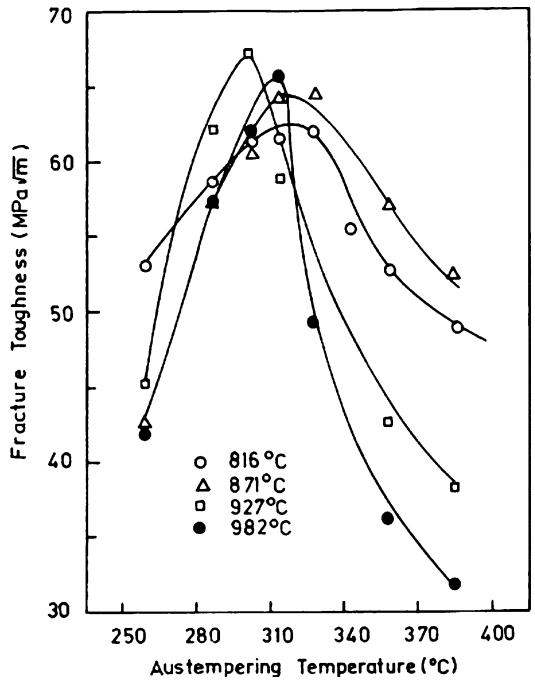

Fig. 7. Influence of the austempering temperature on the fracture toughness at different austenitizing temperatures.

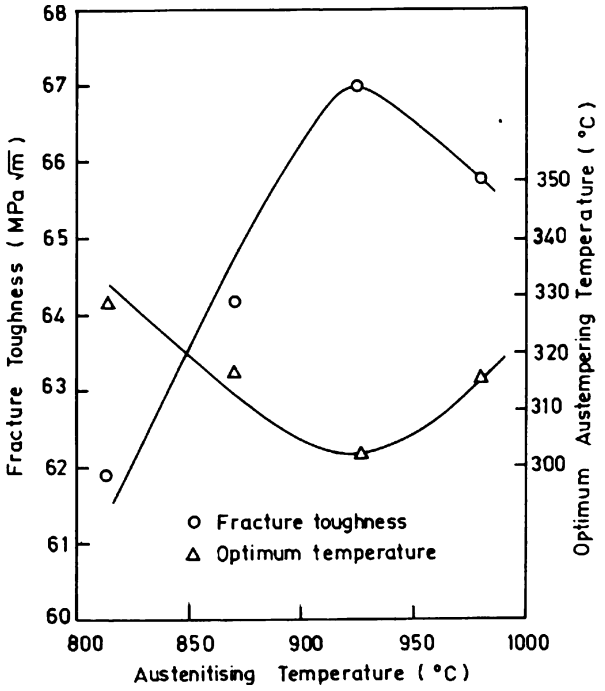

Fig. 8. Influence of the austenitizing temperature on the maximum fracture toughness and the optimum austempering temperature.

curves of the first set are clustered together at relatively low values of austenite and are concave upwards, while those of the second set are clustered together at relatively higher values of austenite content and are concave downwards.

The samples austenitized at the lower temperatures have rather low initial carbon content C_γ. This together with the low diffusion rates of carbon at low temperatures, results in rather low volume fraction of austenite of around 15%. If these are austempered at the higher temperatures, the greater diffusivity of carbon, builds up a high carbon content in austenite ahead of the growing ferrite needles. This results in a large volume fraction of austenite. When the samples are austenitized at higher temperatures, their initial carbon content will be very high. This will help in retaining a large volume fraction of stable austenite at the lower austempering temperatures too, even though the diffusivity of carbon is low. The austenite content will now be similar to those of the samples austenitized at the lower temperatures, but austempered at the higher temperatures. Thus it is seen that the higher austenitizing temperatures are more beneficial at the lower austempering temperatures in increasing the austenite content of the matrix. At the higher austempering temperatures, the decreasing effectiveness of increasing austenitizing temperature can be attributed to the decreasing thermodynamic driving force for the stage I reaction. This is due to the increased initial carbon content of the austenite, and long diffusion distances in the large blocky austenite. Because of this, regions along the prior austenite grain boundaries will not have been stabilized as observed during optical microscopic investigations. It is pertinent to point out here that several investigators [1,6,35] have shown that improved ductility occurs at lower austempering temperatures as the austenitizing temperature is increased. This is attributed to the requirement that the microstructure contain about 25–30 vol.% of austenite. The present results support the contention that this is achieved at lower austempering temperature as the austenitizing temperature is increased.

Table 2
Optimum microstructural features for maximum fracture toughness

Austenitizing temperature (°C)	Fracture toughness (MPa√m)	Optimum austempering temperature (°C)	Morphology of ferrite	Austenite (vol.%)	Carbon content (wt.%)
816	61.90	329	Fine acicular	23.2	1.72
871	64.32	316	Fine acicular	17.8	1.90
927	67.01	302	Fine acicular	21.4	2.16
982	65.81	316	Fine acicular	29.5	1.95

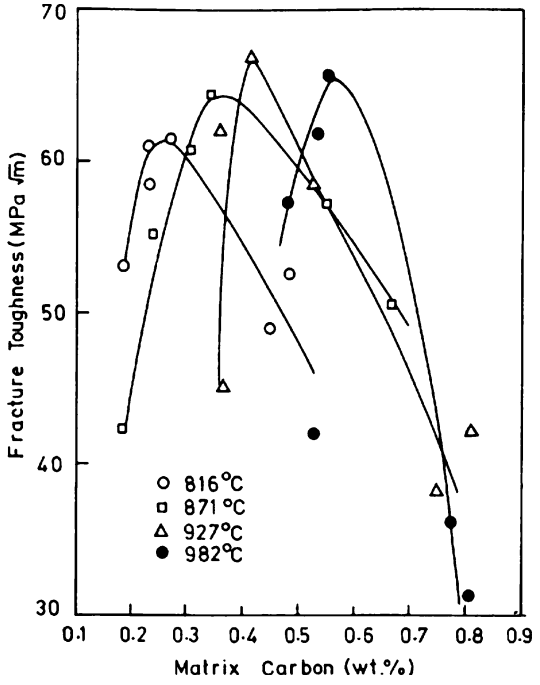

Fig. 9. Influence of the matrix carbon on the fracture toughness.

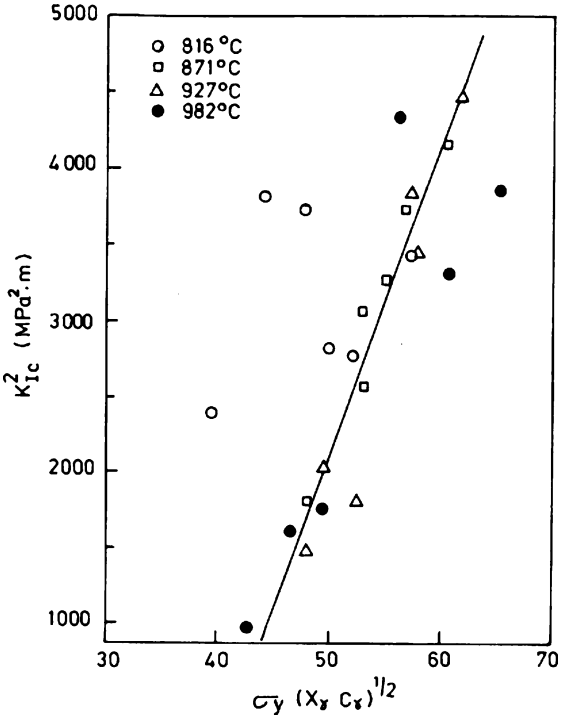

Fig. 10. Plot of K_{IC}^2 against $\sigma_y(X_\gamma C_\gamma)^{1/2}$.

The second important microstructural parameter estimated by X-ray diffraction is the carbon content of the austenite (C_γ). Fig. 5 shows the variation of the carbon content with the austempering temperature at the four austenitizing temperatures. The trend is similar at all four austenitizing temperatures. The carbon content initially rises very rapidly with increasing austempering temperature, attains a maximum value at an intermediate temperature of around 300 °C, and drops gradually with further rise in temperature. This agrees with the previous reports [26–28]. It is also seen from Fig. 5 that the carbon content at a given austempering temperature increases with increasing austenitizing temperature. This can be attributed to the higher initial carbon content of the austenite, which can be calculated approximately by the following expression [36]:

$$C_\gamma^0 = (T_\gamma/420) - 0.17(\mathrm{Si}) - 0.95 \quad (4)$$

where T_γ is the austenitizing temperature in °C and Si is the silicon content in wt.%. Calculations show that the initial carbon contents are (in wt.%) 0.52, 0.65, 0.78 and 0.91 at 816, 871, 927 and 982 °C, respectively. During the transformation reaction, carbon diffuses from the ferrite regions to the surrounding austenite. Assuming that the microstructure consists of only ferrite and austenite, the matrix carbon content can be estimated as $X_\alpha C_\alpha + X_\gamma C_\gamma$ where X_α and X_γ are the volume fractions of ferrite and austenite, respectively, while C_α and C_γ are the respective carbon contents. Taking the carbon content of ferrite as practically zero, the matrix carbon can be approximated as $X_\gamma C_\gamma$. This has been estimated using the X_γ and C_γ values reported in Figs. 4 and 5, and presented in Fig. 6 for different austempering and austenitizing temperatures. At the low austempering temperatures, the matrix carbon is much lower than C_γ. Because of the low diffusion rates and the fast kinetics of ferrite formation, much of the carbon is trapped in the ferrite. However, this will not remain so for long, and will precipitate as carbide. Transmission electron microscopic studies [37,38] have shown that carbides do indeed exist in ferrite in ADIs austempered at low temperatures. As the temperature is raised, increasing diffusivity of carbon ensures increasing matrix carbon. At 357 and 385 °C, the matrix carbon is practically same as C_γ^0 showing that all the carbon in the initial austenite has diffused into the austenite. This is true at all the austenitizing temperatures, with the exception of 982 °C. Here the maximum matrix carbon ($X_\gamma C_\gamma$) was found to be 0.81 wt.%, appreciably lower than the initial carbon content of 0.91 wt.% in austenite (C_γ^0).

The influence of the austenitizing temperature on the microstructure can therefore be summarized as follows:

i) Increasing austenitizing temperature coarsens the microstructure.
ii) Untransformed austenite remains along the prior austenite grain boundaries at high austenitizing and austempering temperatures.
iii) Austenite content generally increases with increasing austenitizing temperature at a given austempering temperature.

Table 3
Tensile properties

Austenitizing temperature (°C)	Austempering temperature (°C)	Yield strength (MPa)	Tensile strength (MPa)
816	260	1155	1269
	288	1185	1277
	302	995	1324
	316	840	1208
	357	744	800
	385	595	706
871	260	1104	1082
	288	1075	1234
	302	1015	1164
	316	1039	1048
	357	731	777
	385	654	738
927	260	819	1082
	288	917	1234
	302	994	1164
	316	802	1048
	357	610	777
	385	558	738
982	260	681	883
	288	878	1146
	302	897	1182
	316	763	941
	357	530	754
	385	479	685

iv) At higher austempering temperatures, the rate of increase in austenite content with austenitizing temperature decreases considerably due to the retention of untransformed austenite.
v) At a given austempering temperature the carbon content of the austenite increases with increasing austenitizing temperature due to the increase initial carbon content.
vi) The matrix carbon content at a given austempering temperature increases with increasing austenitizing temperature, reaching the respective initial carbon contents at high austenitizing temperatures.
vii) At high austenitizing temperatures and high austempering temperatures, the matrix carbon may not reach the initial carbon content because of the retention of the greater fraction of untransformed austenite.

3.2. Fracture toughness

Plane strain fracture toughness tests were carried out on the samples austenitized at the four different temperatures, and subsequently austempered at 260, 288, 302, 316, 357 and 385 °C. For each of these temperatures, five samples were tested, and the fracture toughness values reported are an average of these five tests. Valid K_{IC} values were obtained in all the cases. For the samples austenitized at 816 °C, two additional austempering temperatures were used, namely, 329 and 343 °C, and for the samples austenitized at 982 °C austempering was carried out at 329 °C in addition to the six temperatures mentioned above. Fracture toughness tests were carried out on the samples austempered at these temperatures also.

The influence of the austempering temperature on fracture toughness at the four austenitizing temperatures is shown in Fig. 7. It is found that ADIs with lower ausferritic microstructure have better fracture toughness than those with upper ausferritic microstructure. At a constant austenitizing temperature, the fracture toughness is found to initially increase with increasing austempering temperature, reach a maximum at some intermediate temperature, and drop with further rise in temperature. This matches well with the earlier findings [18,19,26–28] where, also, this kind of dependence of fracture toughness on austempering temperature was observed. Table 2 summarizes the optimum microstructural features for maximum fracture toughness at the four austenitizing temperatures From these it can be concluded that the following microstructural features are essential to obtain maximum fracture toughness:

i) Fine acicular ferrite with austenite present as thin film between the ferrite blades.

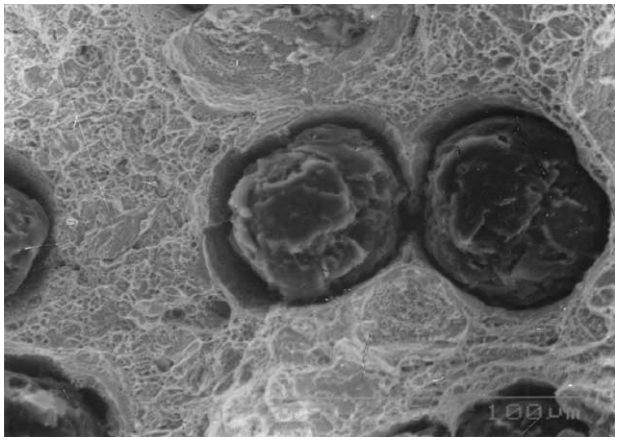

(a)

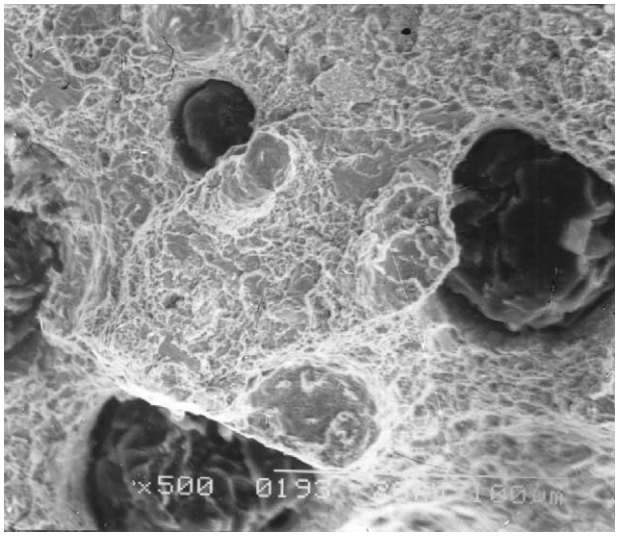

(b)

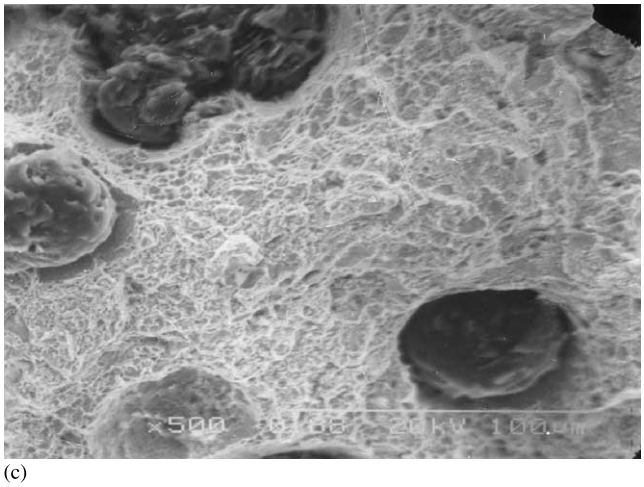

(c)

Fig. 11. (a) Fractographs of samples austenitized at 816 °C and austempered at 260 °C. (b) Fractographs of samples austenitized at 816 °C and austempered at 316 °C. (c) Fractographs of samples austenitized at 816 °C and austempered at 385 °C.

ii) Austenite content of around 25 vol.%.
iii) As high a carbon content as possible in the austenite.
iv) The Higher the carbon content, the better the fracture toughness.

These agree with the conclusions of the previous investigations [26–28]. It was found that, generally as the austenitizing temperature was increased, the optimum austempering temperature shifted to lower values as shown in Fig. 8. From Fig. 4 we find that the austenite content at a given austempering temperature generally increases with increasing austenitizing temperature, because of the higher matrix carbon. Therefore, as the austenitizing temperature is increased the optimum austenite content of 25 vol.% is attained at lower and lower austempering temperatures. However, there was an exception for this general behaviour at the austenitizing temperature of 982 °C. The optimum austempering temperature was found to be 316 °C (for samples austenitized at 982 °C) rather than some value lower than 302 °C. It was further found that as the austenitizing temperature was increased, the maximum fracture toughness increased, as shown in Fig. 8. This can be attributed to the increased matrix carbon, $X_\gamma C_\gamma$. Fig. 9 shows the influence of the matrix carbon on the fracture toughness at the four austenitizing temperatures. Since both X_γ and C_γ increase with increasing austenitizing temperature at a given austempering temperature, the plot of the fracture toughness against the matrix carbon shifts to the right as the austenitizing temperature is increased. This increased matrix carbon is one of the main reasons for the increased fracture toughness.

It has been shown in previous investigations [26,28] that the fracture toughness is maximized when the parameter $\sigma_y(X_\gamma C_\gamma)^{1/2}$ is maximum. The validity of this relationship in the present investigation was examined through the plot of K_2^{IC} against $\sigma_y(X_\gamma C_\gamma)^{1/2}$ as shown in Fig. 10. The yield strength values required for this were determined through tensile tests on samples subjected to different heat treatments, and are reported in Table 3. In Fig. 10, the values corresponding to the austenitizing temperature of 816 °C showed a wide scatter while all the others appeared to be clustered together. A straight line was therefore drawn through the latter points by the method of least squares. This resulted in a straight line with a correlation coefficient of 0.93 showing that above relationship is indeed obeyed in the austenitizing temperature range of 871–982 °C. The non-compliance with this relationship at the austenitizing temperature of 816 °C can be explained as follows:

It was found that at a constant austenitizing temperature, the tensile and yield strengths decreased with decreasing austenitizing temperature in the range 871–982 °C as shown in Table 3. This can be attributed to

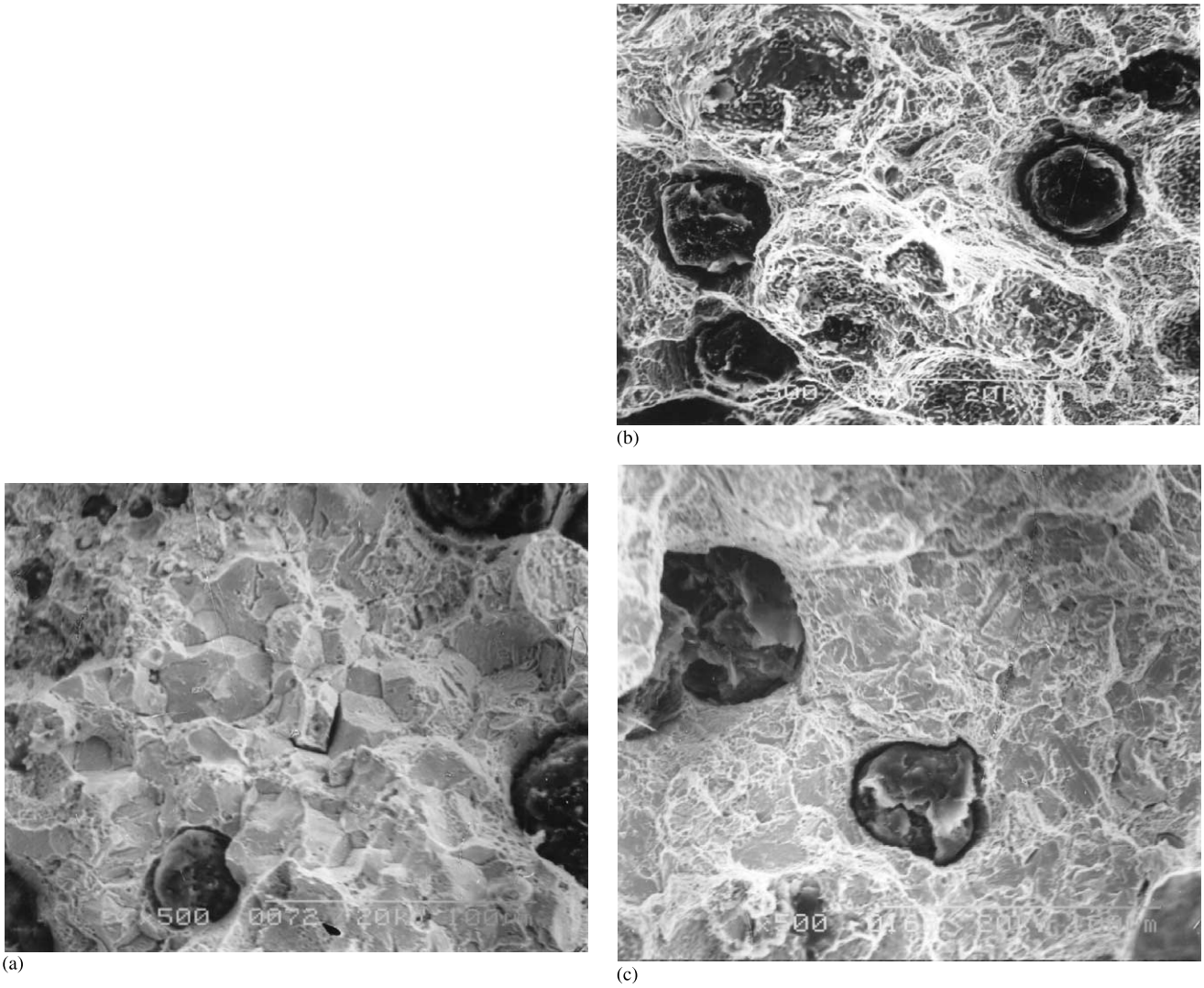

(a) (b) (c)

Fig. 12. (a) Fractographs of samples austenitized at 871 °C and austempered at 260 °C. (b) Fractographs of samples austenitized at 871 °C and austempered at 316 °C. (c) Fractographs of samples austenitized at 871 °C and austempered at 385 °C.

the increasing volume fraction of austenite with increasing austenitizing temperature. As already discussed, at low austempering temperatures like 260–316 °C, the austenite content increases steeply from about 15 to about 30 vol.% when the austenitizing temperature was raised from 871 to 982 °C. A second contributing factor is the increasing coarseness of the microstructure with increasing austenitizing temperature. However, the samples austenitized at 816 °C had low matrix carbon, because of the low initial carbon content, C_γ^0. This effect is not observed at the lowest austempering temperatures of 260 and 288 °C, because in these the strength is primarily decided by the fineness of the ferrite blades. Thus, the lower X_γ, lower C_γ and lower σ_y, together shift the points corresponding to the austenitizing temperature of 816 °C to the left in Fig. 10.

3.3. Fracture mechanism

The fracture surfaces of the compact tension samples were examined by scanning electron microscopy to elicit information on the fracture mechanism. The latter was found to vary considerably with austenitizing and austempering temperatures. At the lowest austenitizing temperature of 816 °C, the fracture mode was predominantly ductile. Transgranular cleavage type of fractures were observed only at the two highest austempering temperatures of 357 and 385 °C. Some typical fractographs are shown in Fig. 11. The results were quite similar when the samples were austenitized at 871 °C. Fig. 12 shows a set of fractographs. Cleavage fractures were observed at austempering temperatures of 260 and 385 °C. At all other austempering temperatures

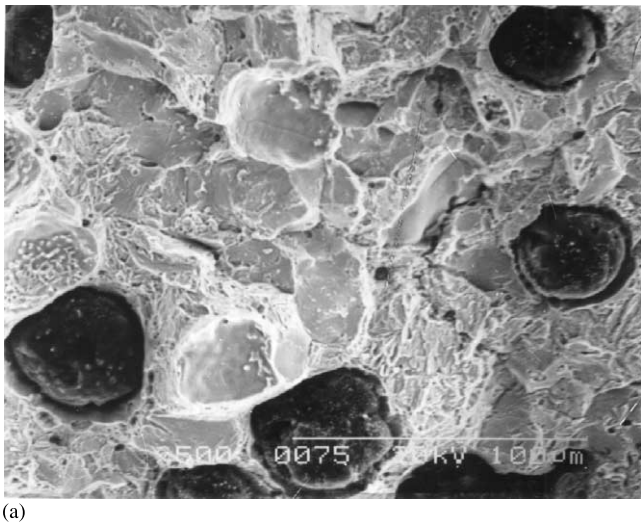

(a)

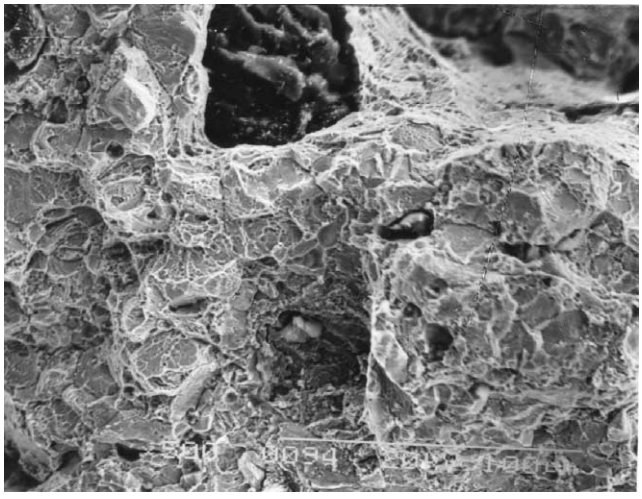

(b)

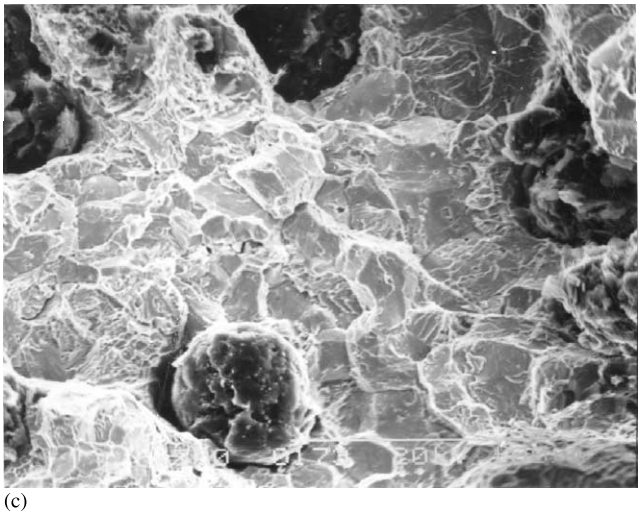

(c)

Fig. 13. (a) Fractographs of samples austenitized at 927 °C and austempered at 260 °C. (b) Fractographs of samples austenitized at 927 °C and austempered at 316 °C. (c) Fractographs of samples austenitized at 927 °C and austempered at 385 °C.

the fracture occurred principally in the dimpled ductile mode. At the next higher austenitizing temperature of 927 °C, fully ductile fracture was confined to the three interrnediate austempering temperatures of 288, 302 and 316 °C. Predominantly cleavage fracture was observed at 260, 357 and 385 °C. The last one also showed some intergranular type of cleavage fracture. Typical fractographs for these samples are shown in Fig. 13. At the highest austenitizing temperature of 982 °C, the fracture was predominantly of the cleavage type. Intergranular type of cleavage fracture was observed at the lowest and highest austempering temperatures. All the others showed transgranular type of cleavage fracture. Some typical fractographs for these samples are presented in Fig. 14. The results of the fractographic investigation are summarized in Fig. 15. This shows the predominant mode of fracture at different combinations of austenitizing and austempering temperatures. The fracture toughness values are also indicated. It was observed that the ductile fracture was generally associated with a fracture toughness of 60 ± 5 MPa$\sqrt{m}$. At lower values of fracture toughness, transgranular type of cleavage fracture was observed upto a fracture toughness of 42 MPa$\sqrt{m}$. At still lower fracture toughness, the fracture mode was predominantly of the intergranular cleavage type. The only exceptions to this general observation were the three intermediate austempering temperatures at the highest austenitizing temperature of 982 °C. These had fracture toughness values in the range of 60 ± 5 MPa$\sqrt{m}$, but exhibited fully transgranular cleavage fracture rather than the dimpled ductile fracture. It is possible that these samples exhibited TRIP phenomenon. It is well known [39,40] that in certain conditions ADI can undergo transformation induced plasticity (TRIP) deformation.

In the presence of a preexisting crack, unstable fracture will occur when a sufficiently large strain is attained at the crack tip. This can be written as [28] as:

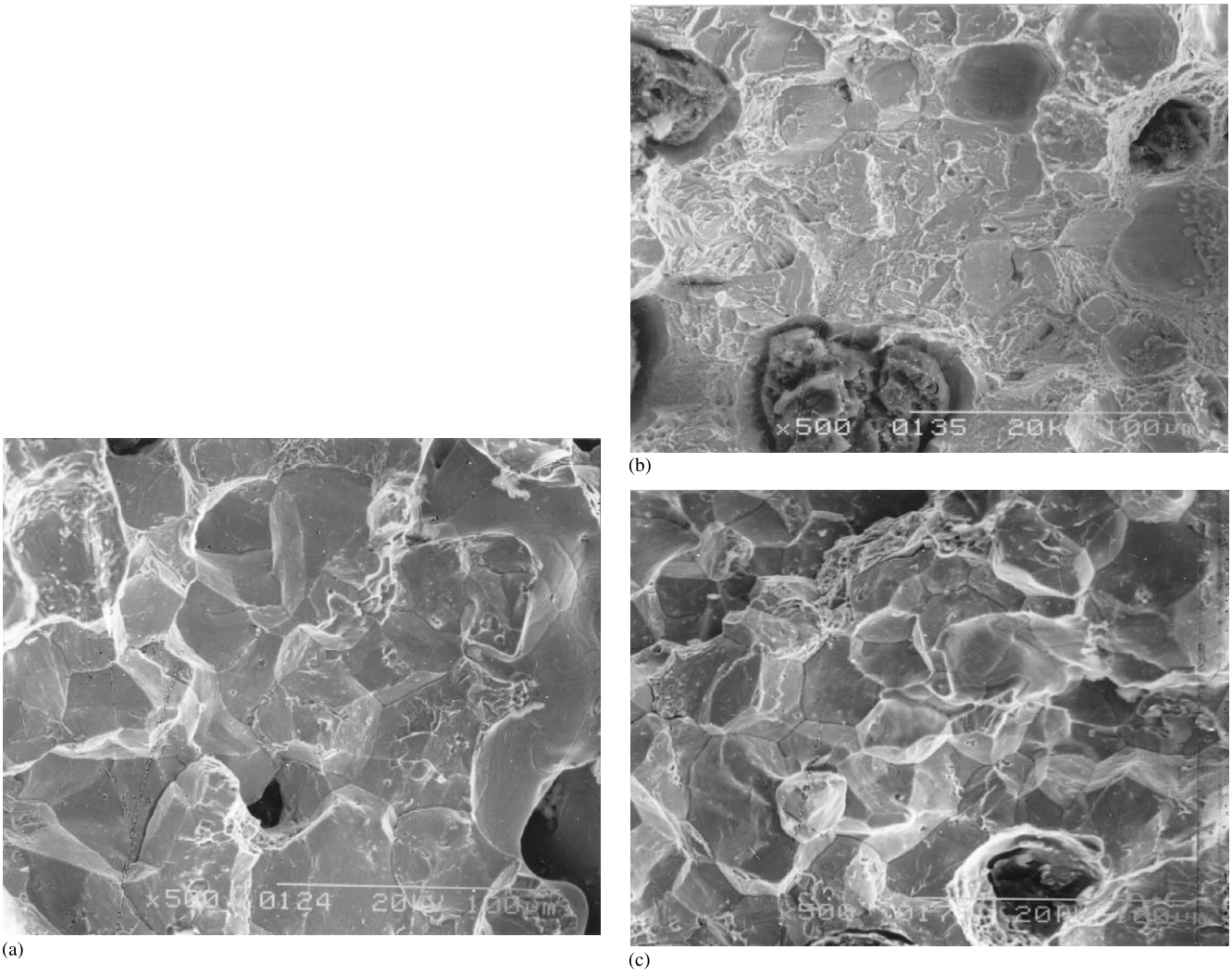

Fig. 14. (a) Fractographs of samples austenitized at 982 °C and austempered at 260 °C. (b) Fractographs of samples austenitized at 982 °C and austempered at 316 °C. (c) Fractographs of samples austenitized at 982 °C and austempered at 385 °C.

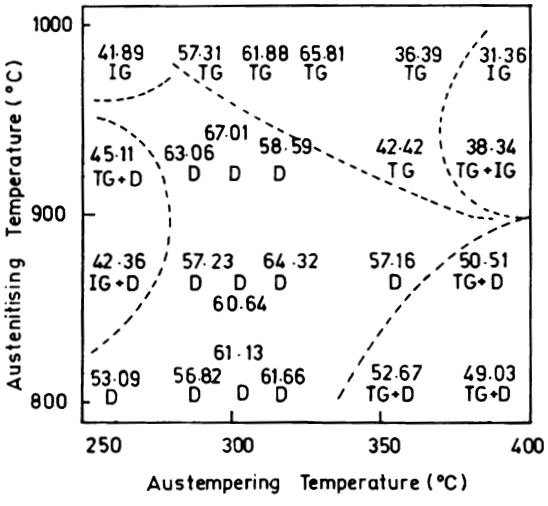

Fig. 15. Influence of austenitizing and austempering temperatures on the fracture mechanism.

$$\varepsilon_f = [K_{IC}^2(I - \upsilon^2)]/[2E\sigma_y\rho] \quad (5)$$

where ε_f is the critical strain at the crack tip for unstable fracture; υ is Poisson's ratio; σ_y is the yield strength of the material; E is the Young's modulus, and ρ is the crack tip radius.

The quantity $K_{IC}^2/E\sigma_y\rho$ on the right hand side in the above equation is a dimensionless quantity, and is hereafter referred to as the toughness parameter. The critical strain at fracture depends on the microstructure, which in turn depends on the heat treatment condition. An analysis of the toughness parameter in terms of the heat treatment will be helpful in understanding the fracture mechanism. The heat treatment condition is expressed in terms of another dimensionless quantity, T_A/T_γ called as the thermal parameter. T_A is the austempering temperature, and T_γ is the austenitizing temperature, both expressed in the absolute scale. The toughness parameter was calculated for each heat treatment condition by taking the corresponding K_{IC}

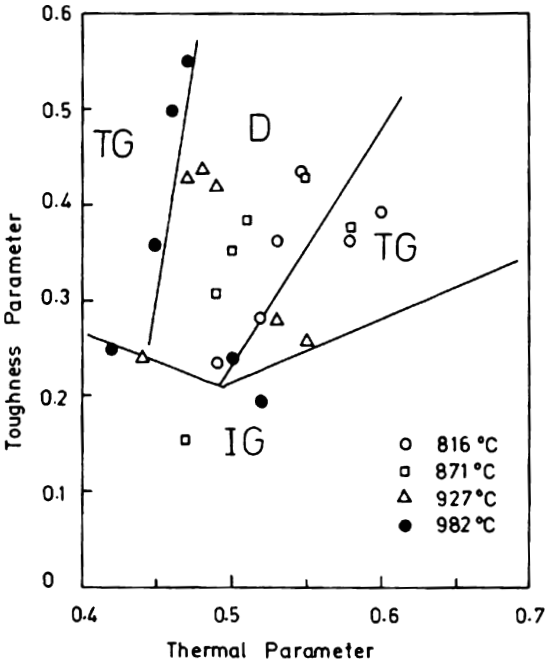

Fig. 16. The plot of the toughness parameter against the thermal parameter.

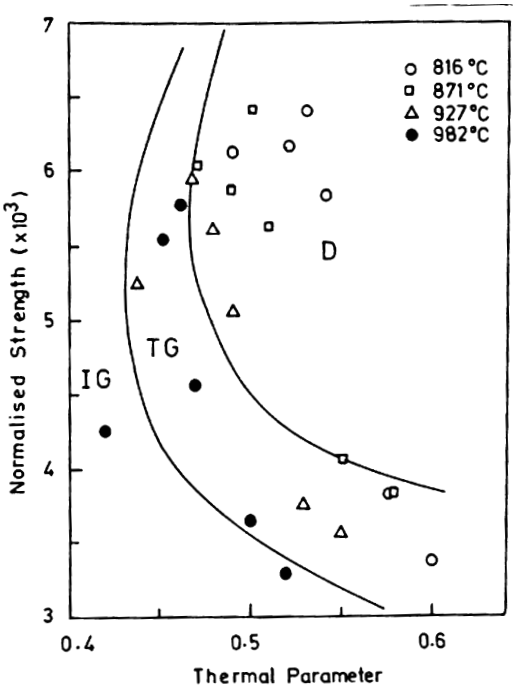

Fig. 17. The plot of normalized strength against the thermal parameter.

and σ_y values. v, E and ρ were assumed to be 0.3, 207 GPa and 50 μm, respectively (reasonable values taken from literature). Fig. 16 is a plot of toughness parameter so calculated against corresponding thermal parameter. The fracture mechanisms observed under the different heat treatment conditions described earlier, and presented in Fig. 15 are also indicated on this figure. Boundaries were drawn between regions of different fracture mechanisms. This shows possible fracture mechanisms under various combinations of toughness and thermal parameters. At a constant thermal parameter, toughness parameter can vary widely and so also, the fracture mechanism. This is because, for various combinations of T_A and T_γ at a constant T_A/T_γ, the microstructure can vary considerably. Similarly, at a constant toughness parameter, the fracture mechanism can vary considerably because T_A/T_γ can vary widely. The figure shows that the dimpled ductile fracture that is associated with best fracture toughness is observed when the thermal parameter is around 0.5.

Cast irons are generally classified on the basis of their tensile strengths. Therefore, an analysis of the fracture mechanism based on the tensile strength would be of considerable practical significance. Fig. 17 shows a plot of normalized strength, σ/E, against the thermal parameter, T'_A/T_γ, under various heat treatment conditions in the present investigation. The predominant fracture mechanism in each case is also indicated on the diagram. Two curves are drawn demarcating the different mechanisms of fracture. To the right of curve C_1 the fracture is mainly dimpled ductile, while to the left it is mainly of the transgranular cleavage type. The diagram indicates that when T_A/T_γ is less than 0.48, it is unlikely that fracture can be of the dimpled ductile type.

4. Conclusions

1. Irrespective of the austenitizing temperature, ADIs with lower ausferritic microstructure exhibit better fracture toughness than those with upper ausferritic microstructure.
2. At all austenitizing temperatures the fracture toughness is maximized when the microstructure consists of about 25 vol.% of austenite that is present as thin slivers between fine bainite blades. The carbon content of the austenite should be as high as possible, and not less than 1.8 wt.%.
3. The optimum austempering temperature for maximum fracture toughness decreases with increasing austenitizing temperature.
4. K_{IC}^2 is generally proportional to $\sigma_y(X_\gamma C_\gamma)^{1/2}$. Deviations from this general rule occur at very low austenitizing temperatures due to the low matrix carbon.
5. Dimpled fracture that is associated with high fracture toughness occurs when thermal parameter is about 0.5 and the toughness parameter is greater than 0.3. It is unlikely that good fracture toughness can be attained when the thermal parameter is less than 0.48.

Acknowledgements

This work was carried out when the first author (PPR) spent two years at Wayne State University as a visiting scientist. The work was financially supported by Ford Motor Company, Dearborn, Michigan.

References

[1] R.B. Gundlach, J.F. Janowak, Met. Progr. 128 (2) (1985) 19–26.
[2] R.B. Gundlach, J.F. Janowak, AFS Trans. 91 (1983) 377–388.
[3] G. Wilkinson, C. Grupke, Second International Conference: on Austempered Ductile Iron, Ann Arbor, MI, March 1986, American Foundrymen's Society, Des Plaines, IL, 1991, pp. 349–358.
[4] J. Panasiewicz, C. Grupke, J. Huth, Proc.World Conf. on Austempered Ductile Iron, Bloomingdale, IL, Mar. 1991, American Foundrymen's Society, Des Plaines, IL, 1991, pp. 176–194.
[5] K. Okazakie, H. Asai, M. Tokuyoshi, H. Kusumoki, H. Sakamura, Proc. World Conf. on Austempered Ductile lron, Bloomingdale, IL, Mar. 1991, American Foundrymen's Society, Des Plaines, IL, 1991, pp. 288–299.
[6] R.A. Harding, G.N.J. Gilbert, Br. Foundryman 79 (1986) 489–496.
[7] I. Schmidt, Z. Metallkd. 75 (1984) 747–751.
[8] S.M. Shah, J.D. Verhoeven, Wear 113 (1986) 267–273.
[9] I. Schmidt, A. Schuchert, Z. Metallkd. 78 (1987) 871–876.
[10] L. Bartosiewicz, A.R. Krause, F.A. Alberts, I. Singh, S.K. Putatunda, Mater. Charact. 30 (1993) 221–234.
[11] P. Shamugam, P.P. Rao, K.R. Udupa, N. Venkataraman, J. Mater. Sci. 29 (1994) 4933–4940.
[12] K. Zum Ghar, B.L. Wagner, Arch. Eisenhutenwes. 50 (1979) 269–274.
[13] G. Barbezat, H. Mayer, Sulzer Tech. Rev. 2 (1986) 32–38.
[14] S.C. Lee, C.C. Lee, AFS Trans. 96 (1988) 827–838.
[15] J. Aranzabal, I. Gutierez, J.M. Rodriguez-lbabe, J.J. Urcola, Mater. Sci. Technol. 8 (1992) 263–273.
[16] L. Bartosiewicz, I. Singh, F.A. Alberts, A.R. Krause, S.K. Putatunda, J. Mater. Eng. Perform. 4 (1995) 90–101.
[17] S.K. Putatunda, I. Singh, J. Test. Eval. 23 (1995) 325–332.
[18] E. Dorazil, B. Barta, E. Muntsorova, L. Stransky, A. Huvar, AFS Int. Cast Met. J. 7 (1982) 52–58.
[19] D.J. Moore, T.N. Rouns, K.B. Rundman, AFS Trans. 93 (1985) 705–714.
[20] T.N. Rouns, K.B. Rundman, D.M. Moore, AFS Trans. 92 (1984) 815–840.
[21] N. Darwish, R. Elliot, Mater. Sci. Technol. 9 (1993) 882–889.
[22] P.P. Rao, S.K. Putatunda, Metall. Mater. Trans. A 28A (1997) 1457–1470.
[23] N. Darwish, R. Elliot, Mater. Sci. Technol. 9 (1993) 586–602.
[24] H. Bayati, R. Elliot, G.W. Lorimer, Mater. Sci. Technol. 11 (1995) 776–786.
[25] A.S. Hamid Ali, R. Elliot, Mater. Sci. Technol. 12 (1996) 1021–1031.
[26] P.P. Rao, S.K. Putatunda, Mater. Sci. Technol. 14 (1998) 1257–1265.
[27] S.K. Putatunda, R. Gupta, P.P. Rao, Understanding Microstructure: Key to Advances in Materials, Proceedings of the 25th Annual Technical Meeting of the International Metallographic Society, International Metallographic Society, Columbus, OH, 1996, pp. 103–110.
[28] P.P. Rao, S.K. Putatunda, Metall. Mater. Trans. A 29A (1998) 3005–3016.
[29] K.L. Hayrynen, D.J. Moore, K.B. Rundman, AFS Trans. A 98 (1990) 47–180.
[30] A.S.H. Ali, K.I. Uzlov, N. Darwish, R. Elliot, Mater. Sci. Technol. 10 (1994) 35–45.
[31] R.C. Klug, M.B. Hintz, K.B. Rundman, Metall. Mater. Trans. A 16A7 (1985) 797–805.
[32] J.L. Doong, C.H. Chen, Fat. Fract. Eng. Mater. Struct. 12 (1989) 155–165.
[33] ASTM E-8, Annual Book of ASTM Standards, ASTM, Philadelphia, Vol 0.3.01, 1998, pp. 545–566.
[34] ASTM E-399, Annual Book of ASTM Standards, ASTM, Philadelphia, Vol 0.301, 1998, pp. 745–766.
[35] J. Dodd, Mod. Cast. 68 (5) (1978) 60–66.
[36] R.C. Voigt, C.R. Loper, Proc. Ist Int. Co'Â on Austempered Ductile Iron, ASM, Metals Park, OH, 1984, pp. 83–84.
[37] L. Sidjanin, R.E. Smallman, Mater. Sci. Technol. 8 (1992) 1095–2006.
[38] L. Sidjanin, R.E. Smallman, S.M. Boutorabi, Mater. Sci. Technol. 10 (1994) 711–723.
[39] J. Vuorinen, Proceedings of the 2nd International Conference on Austemered Ductile Cast Iron, Ann Arbor, Michigan, 1986, pp. 179–188.
[40] P. Mayr, H. Vetters, J. Walla, Investigations on the Stress Induced Martensite Formation in Austempered Ductlile Cast Iron (ADI). Proceedings of the 2nd International Conference on Austempered Ductile Cast Iron, Ann Arbor, MI, 1986, pp. 171–178